

A. CWUDZIŃSKI\*<sup>‡</sup>**CHEMICAL HOMOGENIZATION OF LIQUID STEEL FLOWED THROUGH CONTINUOUS CASTING SLAB TUNDISH DURING ALLOYING PROCESS****CHOMOGENIZACJA CHEMICZNA CIEKŁEJ STALI PRZEPLYWAJĄCEJ PRZEZ KADŹ POŚREDNIĄ PODCZAS PROCESU WPROWADZANIA DODATKU STOPOWEGO**

This paper presents the results of research on the behaviour of an alloy addition in steel flowing through the tundish used for casting slabs. The device under examination is a wedge-shaped single-nozzle tundish of a capacity of 30 Mg. Due to the complexity of alloy addition dissolution and dispersion in metallurgical processes, a decision was made to use the Species Model available within the Ansys-Fluent<sup>®</sup> program. For describing the turbulence, the Realizable k- $\epsilon$  model was chosen. By defining the heat losses on respective planes making up the virtual model, the non-isothermal conditions existing during the flow of liquid steel through the tundish were considered. From the performed numerical simulations, the fields of steel flow and steel temperature and alloy addition concentration in the tundish working space were obtained. In order to accurately illustrate the process of chemical homogenization in the tundish working space, mixing curves were recorded. Based on the obtained results (mixing curves), the mixing time needed for achieving the 95% level of chemical homogenization was calculated.

*Keywords:* tundish, steel flow, numerical modeling, chemical homogenization, alloy addition

Praca przedstawia wyniki badań zachowania się dodatku stopowego w stali przepływającej przez kadź pośrednią stosowaną do odlewania wlewków płaskich. Rozpatrywanym obiektem jest jedno-wylewowa kadź pośrednia o kształcie klina i pojemności nominalnej 30 Mg. Do opisu zachowania się dodatku stopowego w ciekłej stali zastosowano model "Species" dostępny w programie Ansys-Fluent<sup>®</sup>. Do opisu turbulencji zastosowano model Realizable k- $\epsilon$ . Poprzez zdefiniowanie strumieni ciepłych na poszczególnych płaszczyznach wirtualnego modelu otrzymano przepływ ciekłej stali przez kadź pośrednią w warunkach nieizotermicznych. Na podstawie wykonanych symulacji numerycznych otrzymano pola przepływu i temperatury ciekłej stali oraz rozkładu stężenia dodatku stopowego. W trakcie symulacji numerycznej zarejestrowano również krzywe mieszania. Na podstawie krzywych mieszania wyznaczono czas mieszania wymagany do osiągnięcia 95% poziomu homogenizacji chemicznej.

**1. Introduction**

Continuous steel casting is a technology commonly used for production of steel semi-finished products. The possibility of controlling the casting speed and cooling intensity creates an opportunity to cast both carbon and alloy steel grades [1-4]. The dynamic growth of the automotive, armaments, shipbuilding, mining or extractive industries has spurred the search for new steel grades. Thus steels resistant to wear during operation in aggressive environmental conditions, e.g. low temperatures and high pressures, have been developed. In the production of alloy steels, Ni, Cr, Al, Si, Mo, Co, Ti, Nb, V, W, Zr or Cu are introduced in varying configurations and quantities. The alloys additions are introduced during secondary metallurgical treatment on the ladle furnace stand. In addition, during the ladle furnace treatment, the metal purity required for alloy steels, as measured by low contents of sulphur, non-metallic inclusions and gases, is obtained [5-8]. However, achieving the 95% of

chemical homogenization of steel, its refining and heating up to the casting temperature will require energy and time. Therefore, alternative technological solutions to introducing selected alloy additions to steel could intensify the production process, while reducing the costs. After the ladle furnace treatment, the liquid steel is cast by a continuous method. From the steel-making ladle, the liquid steel is poured into the tundish, where it will stay for a specific period of time. Then the liquid steel flows into the mould, in which the process of solidification and concast slab formation starts. The continuous liquid steel movement in the tundish working space is intensified by the feeding stream. The process of steel mixing within the tundish working space can be additionally modified by flow control devices, such as a dam, a weir, a subflux turbulence controller or a gas-permeable barrier [9-12]. In view of the above, the specific time of liquid steel residence in the tundish and the feeding stream mixing energy create a possibility of effective introducing alloy additions to liquid steel during continuous

\* DEPARTMENT OF METALS EXTRACTION AND RECIRCULATION, FACULTY OF PRODUCTION ENGINEERING AND MATERIALS TECHNOLOGY, CZESTOCHOWA UNIVERSITY OF TECHNOLOGY, 19 ARMII KRAJOWEJ AV., 42-200 CZESTOCHOWA, POLAND

<sup>‡</sup> Corresponding author: cwudzinski@wip.pcz.pl

casting, with the 95% level of chemical homogenization being achieved. This paper presents the results of research on the behaviour of an alloy addition in steel flowing through the tundish used for casting slabs.

## 2. Characterization of the test facility and computing methodology

The device under examination is a wedge-shaped single-nozzle tundish of a capacity of 30 Mg. The tundish being currently operated in industry is only equipped with a low ( $h=120$  mm) dam with two overflow windows (Fig. 1). Two different tundish bottom levels provide a metal head of 0.7 m in the tundish pouring zone and 0.92 m in the stopper rod system zone. Argon is blown through the ceramic stopper rod. The stopper rod controls the flow rate of steel flowing out from the tundish to the mould. The inert gas assures the stabilization of the liquid steel flow and prevents the process of submerged entry nozzle clogging. The liquid metal flows into the tundish via the ceramic ladle shroud. The free liquid steel surface is protected against the action of external factor by tundish powder and a fibreboard panel. Figure 1 shows a virtual tundish model with indicated measurement points and the location of alloy addition feeding to the liquid steel (numerical simulation). Measurement points are positioned at different zones in the tundish working space to obtain a complete picture of the alloy addition dispersing within the liquid steel.

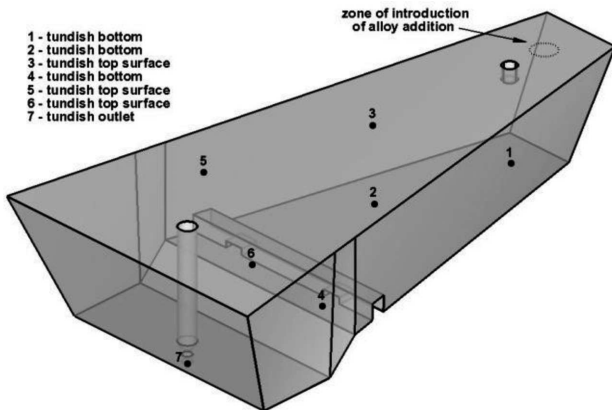


Fig. 1. Tundish virtual model with measurement points

Computer simulation of the liquid steel flow and alloy addition behaviour in turbulent motion conditions was done using the Ansys-Fluent<sup>®</sup> computer program. The basic mathematical model equations describing the phenomena under examination are as follows:

$$\frac{\partial \rho}{\partial t} + \nabla(\rho u) = 0 \quad (1)$$

$$\frac{\partial}{\partial t}(\rho u) + \nabla(\rho u u) = -\nabla p + \nabla(\bar{\tau}) + \rho g \quad (2)$$

$$\frac{\partial}{\partial t}(\rho E) + \nabla(u(\rho E + p)) = \nabla \left( k_{eff} \nabla T - \sum_j h_j J + (\bar{\tau}_{eff} u) \right) \quad (3)$$

$$(\rho - \rho_0)g \approx -\rho_0 \beta (T - T_0)g \quad (4)$$

For describing the turbulence motion of liquid steel and nickel alloy, the realizable  $k-\varepsilon$  model was adopted. In the realizable  $k-\varepsilon$  turbulence model, constants take on the following values:  $C_2 = 1.9$ ,  $\sigma_k = 1.0$ ,  $\sigma_\varepsilon = 1.2$  [13]. Interactions between the liquid steel and the inert gas (Ar) were simulated using the Discrete Phase Model (DPM). The effects of the chaotic behaviour of bubbles in the volume of liquid steel are described by the discrete random walk model (equation 6).

$$\frac{du_B}{dt} = \frac{18\mu C_D Re}{24\rho_B d_B^2} (u - u_B) + \frac{g(\rho_B - \rho)}{\rho_B} + \frac{1}{2} \frac{\rho}{\rho_B} \frac{d(u - u_B)}{dt} \quad (5)$$

$$u'_B = \zeta \sqrt{\frac{2k}{3}} \quad (6)$$

Due to the complexity of alloy addition dissolution and dispersion in metallurgical processes, a decision was made to use the Species Model available within the Ansys-Fluent<sup>®</sup> program.

$$\frac{\partial}{\partial t}(\rho Y_i) + \nabla(\rho u Y_i) = -\nabla J \quad (7)$$

where:  $u$  – liquid steel velocity, m/s,  $\rho$  – liquid steel density,  $\text{kg/m}^3$ ,  $t$  – time, s,  $p$  – pressure, Pa,  $g$  – gravitational acceleration,  $\text{m/s}^2$ ,  $\bar{\tau}$  – stress tensor, Pa,  $\bar{\tau}_{eff}$  – effective stress tensor, Pa,  $T$  – temperature, K,  $\mu$  – viscosity, Pa·s,  $E$  – energy, J,  $k_{eff}$  – effective thermal conductivity, W/m·K,  $J$  – diffusion flux,  $\text{kg/m}^2\cdot\text{s}$ ,  $u_B$  – velocity of bubble, m/s,  $C_D$  – drag coefficient,  $\rho_B$  – density of bubble,  $\text{kg/m}^3$ ,  $Re$  – Reynolds number,  $d_B$  – diameter of bubble, m,  $u'_B$  – bubble random velocity fluctuation, m/s,  $k$  – kinetic energy of turbulence,  $\text{m}^2/\text{s}^2$ ,  $\zeta$  – random number,  $Y_i$ : local mass fraction of each species.

The liquid metal flows through the tundish at a mass flow rate of 34.43 kg/s. The parameters  $k$  and  $\varepsilon$ , as defined for the steel flowing into the tundish, were  $0.017161 \text{ m}^2/\text{s}^2$  and  $0.064231 \text{ m}^2/\text{s}^3$ , respectively. By defining the heat losses on respective planes making up the virtual model, the non-isothermal conditions existing during the flow of liquid steel through the tundish were considered. The temperature of the liquid steel flowing into the tundish was 1823 K. The heat loss flux was  $-2600 \text{ W/m}^2$  on the tundish walls and bottom and  $-15000 \text{ W/m}^2$  on the free steel table surface. The liquid steel properties are as follows: density,  $7010 \text{ kg/m}^3$ ; viscosity,  $0.007 \text{ Pa}\cdot\text{s}$ ; heat capacity,  $750 \text{ J}\cdot\text{kg/K}$ ; thermal conductivity,  $41 \text{ W/m}\cdot\text{K}$ ; steel thermal expansion coefficient,  $0.0001 \text{ 1/K}$ . The liquid nickel properties are as follows: density,  $7650 \text{ kg/m}^3$ ; viscosity,  $0.0047 \text{ Pa}\cdot\text{s}$ ; heat capacity,  $556 \text{ J}\cdot\text{kg/K}$ ; thermal conductivity,  $50 \text{ W/m}\cdot\text{K}$ . The mass diffusivity of nickel in the steel is  $5.35\text{e-}09 \text{ m}^2/\text{s}$  [14-15]. The alloy addition was introduced to the liquid steel in a continuous manner at a rate of  $0.386 \text{ kg/s}$ . Argon was blown in to the liquid steel at a flow rate of  $4 \text{ Nl/min}$ . The free steel table surface was described using the boundary condition of a wall with zero stresses. The virtual object was built of 470,000 tetrahedral elements. All numerical simulations were done by employing a double-precision solver (3ddp) using discretization of the second order. For describing the velocity and pressure fields, the Simplec algorithm was selected. The correctness of the results obtained with the “Species” numerical model were verified using a numerical model, a physical model and an industrial experiment [16-18]. The average time of liquid steel residence in the tundish is 736

sec. The dimensionless time (DT) was calculated as the ratio of the current time to the average time of steel residence in the tundish. The casting of a single steel melt lasts 4 DT. The dimensionless concentration of the alloy addition in the liquid steel was calculated from the relationship (8) [19-21]:

$$C = \frac{C_t - C_0}{C_r - C_0} \quad (8)$$

where:  $C_t$  – temporary alloy concentration,  $C_0$  – initial alloy concentration,  $C_r$  – required alloy concentration.

### 3. Results and Discussion

From the performed numerical simulations, the fields of steel flow and temperature and alloy addition in the tundish working space were obtained. Upon flowing into the tundish, the main steel stream hits the bottom and then flows around towards the rear wall, the side walls and the low dam, forming intermediate streams and a main stream feeding the tundish nozzle (Fig. 2a). The intermediate stream flowing towards the rear wall continues along this wall heading for the free surface, and then falls down along the main feeding stream to form a steel circulation zone. The steel streams flowing towards the side walls form another flow patterns oriented to the tundish axis and in the stopper rod direction. The liquid steel streams oriented to the tundish axis descend in the central tundish part towards the bottom. They form a liquid steel circulation zone lying in the plane transverse to the tundish axis. Before dam (as seen from the tundish pouring zone), the flow direction of part of the streams descending towards the bottom is modified by the reverse streams flowing in the pouring zone direction. As a result of the reverse streams and the intermediate feeding streams meeting, a steel circulation zone forms at the bottom in the central tundish part (Fig. 2a). The intermediate feeding streams forming the steel circulation zone are part of the main feeding stream which, upon flowing into the tundish, has been partially dispersed and directed towards the dam (Fig. 2a). Whereas after the dam (as seen from the stopper rod system zone), the liquid steel streams flow towards the nozzle. Part of the intermediate streams flowing along the side wall rise towards the free surface (Fig. 2b). Upon reaching the stopper rod zone, the intermediate streams descend towards the tundish nozzle in the immediate vicinity of the front tundish wall and the stopper rod (Fig. 2a and Fig. 2b). In this stopper rod system region, between the bottom and the front side and the side walls, a steel circulation zone is formed (Fig. 2b). Figures 2c and 2d show a vertical split of the liquid steel temperature isolines both in the central zone and in the zones located close to the side walls. The difference in liquid steel temperature value between the pouring zone and the stopper rod system zone was 4 K, which indicates the thermal stability of the facility. Figures 3a to 3d represent maps of variations in the concentration of the alloy addition in the liquid steel during casting. After a time period of 0.65 DT, the highest alloy addition concentration was recorded in the zone of alloy addition introduction to the tundish. In contrast, the lower concentration occurred at the tundish bottom (the stopper rod zone), which confirms the hydrodynamic pattern and flow directions of the stream feeding the tundish. Due to the similar

steel densities and the alloy addition used, the process of alloy addition spreading out in the liquid steel is closely related to the steel motion. After 1.35 DT, the alloy addition concentration in the space between the pouring zone and the stopper rod system zone starts equalizing (Fig.3b, 3c and 3d). However, even after 2.71 DT, the alloy addition concentration in individual regions of the central tundish part remains varying. This evidences the complexity of the chemical homogenization process during continuous casting.

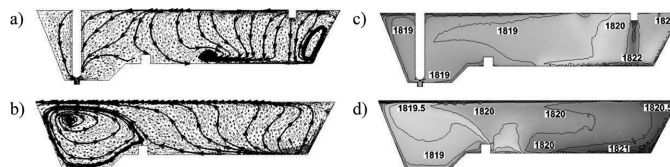


Fig. 2. Direction of liquid steel flow: a) central plane of tundish, b) plane near longitudinal side wall, temperature of liquid steel: c) central plane of tundish, d) plane near longitudinal side wall

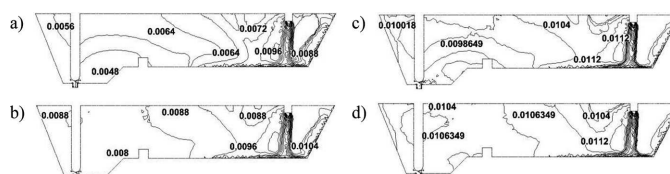


Fig. 3. Fields of alloy addition concentration on the central plane: a) after 0.65 DT, b) after 1.35 DT, c) 2.03 DT, d) 2.71 DT

In order to accurately illustrate the process of chemical homogenization in the tundish working space, mixing curves were recorded. Based on the obtained results (mixing curves), the mixing time needed for achieving the 95% level of chemical homogenization was calculated. The working space was divided into four zones: Zone 1 of pouring (measurement point no.1), Zone 2 located in the mid-distance between the pouring location and the dam (measurement points no.2 and no.3), Zone 3 of the dam (measurement points no.4 and no.5), and Zone 4 of the stopper rod system (measurement points no.6 and no.7). Figure 4 shows mixing curves recorded at seven measurement points. The time that elapses between the moment of introducing the alloy addition to the liquid steel and recording its presence at selected measurement points confirms the direction of flow of the main feeding stream. After 0.001 DT, the alloy addition comes up in the tundish pouring zone in the feeding stream axis. Then, after 0.0115 DT, the alloy addition was recorded at the second measurement point. Reaching the third measurement point took the alloy addition a time of 0.0217 DT. Further on, the alloy addition is transferred by the liquid steel, successively, to the fifth, sixth, seventh and fourth measurement points after a time of 0.038, 0.051, 0.109 and 0.161 DT, respectively. To sum it up, the alloy addition behaviour is consistent with the flow directions of the main feeding stream which, after hitting the tundish bottom, flows over the bottom towards the side walls and then, in the immediate vicinity of the side walls, it assumes an ascending character, heading for the free surface. Only after reaching the front tundish wall does the main stream fall down towards the tundish nozzle. The recorded order of the alloy addition showing up in selected tundish zones shows that the process of

alloy addition dispersion within the steel is dependent on the flow directions of steel streams. Attaining a homogenization level of 95% in the tundish steel requires a specific time. For the pouring zone and the first measurement point, the force of the feeding stream and its permanent flow from the steel-making ladle prevents the 95% chemical homogenization level from being quickly attained, since after the entire time of melt casting had elapsed, the maximum dimensionless alloy addition concentration amounted to 0.64. The required chemical homogenization level was achieved in tundish Zone 2. The alloy addition mixing time was 1.66 and 2 DT, respectively, for measurement points 3 and 2. After 2.05 DT, the required homogenization level was also attained at measurement point 5. However, at point 4 located, similarly as point 5, also in Zone 3, the mixing time was 3.81 DT. The extended time needed for attaining the 95% homogenization level is due to the formation of stagnant flow zones within the volume of liquid steel. The steel circulation hampers the processes of mass exchange between the circulation zone and the streams dynamically flowing around it, which are alloy addition carriers. A similar mixing time value of 3.79 DT was recorded at measurement point 6, also located in the immediate vicinity of liquid steel circulation zone influence, as shown in Figure 2b. For continuous casting it seems most important to attain the 95% chemical homogenization level at the tundish nozzle, as the steel flows through the nozzle to the mould, where the concast slab formation process starts. Hence, the steel flowing to the mould should be characterized by chemical composition required for a given steel grade. The mixing time at the measurement point located at the tundish nozzle amounted to 2.82 DT. Thus, with this alloy addition feeding technique and for the casting conditions under examination, after casting the  $\frac{3}{4}$  of the first heat mass in the casting sequence, the 95% level of chemical homogenization of steel flowing to the mould can be achieved.

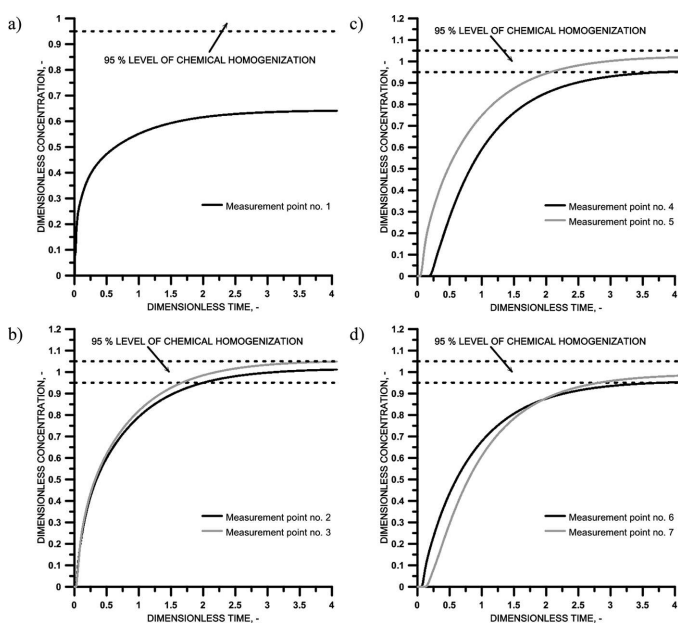


Fig. 4. Mixing curve: a) measurement point no. 1, b) measurement points no. 3 and 4, c) measurement points no. 4 and 5, d) measurement points no. 6 and 7

#### 4. Summary

From the performed computer simulations it can be found that:

- the one-strand slab tundish under examination is a flow reactor in which the feeding stream is split into streams supplying the nozzle and the circulation movement zones,
- the average liquid steel residence time and the hydrodynamic pattern being the result of tundish working space influence on the feeding zone allow the alloy addition to be effectively introduced to the liquid steel during the CSC process,
- the speed and directions of alloy addition dispersion within the liquid steel depend on the hydrodynamic pattern of its flow in the tundish,
- for the examined tundish furniture variant and the considered conditions of both casting and alloy addition introduction, attaining the 95% chemical homogenization level of the steel at the nozzle requires 2.82 DT.

#### Acknowledgements

This scientific work has been financed from the resources of National Science Centre in the years 2011-2014 as Research Project No. N508622740.

#### REFERENCES

- [1] W. Derda, J. Wiedermann, *Archiv. of Metall. and Mater.* **57**, 303-310 (2012).
- [2] A. Sorek, Z. Kudliński, *Archiv. of Metall. and Mater.* **57**, 371-377 (2012).
- [3] A. Burbelko, J. Falkus, W. Kapturkiewicz, K. Sołek, P. Drożdż, M. Wróbel, *Archiv. of Metall. and Mater.* **57**, 379-384 (2012).
- [4] M. Rywotycki, K. Miłkowska-Piszczek, L. Trębacz, *Archiv. of Metall. and Mater.* **57**, 385-393 (2012).
- [5] D. Mazumdar, R.I.L. Guthrie, *ISIJ Int.* **35**, 1-20 (1995).
- [6] M. Chen, N. Wang, Y. Yao, J. Geng, K. Xiong, *Steel Res. Int.* **78**, 468-472 (2007).
- [7] B. Zdonek, I. Szypuła, J. Kozłowski, S. Szczęch, *Archiv. of Metall. and Mater.* **57**, 347-353 (2012).
- [8] B. Kalandyk, W. Wojtal, *Archiv. of Metall. and Mater.* **58**, 779-783 (2013).
- [9] J. Falkus, J. Lamut, *Archiv. of Metall. and Mater.* **50**, 709-718 (2005).
- [10] A. Cwudziński, J. Jowśa, *Archiv. of Metall. and Mater.* **53**, 749-761 (2008).
- [11] A. Cwudziński, *Ironmaking Steelmaking* **37**, 169-180 (2010).
- [12] T. Merder, J. Pieprzyca, *Steel Res. Int.* **83**, 1029-1038 (2012).
- [13] T.-H. Shih, W.W. Liou, A. Shabbir, Z. Yang, J. Zhu, *Comput. Fluid* **24**, 227-238 (1995).
- [14] R.I.L. Guthrie, *Engineering in Process Metallurgy*, Clarendon Press Oxford 1992.
- [15] T. Iida, R.I.L. Guthrie, *The physical properties of liquid metals*, Clarendon Press Oxford 1993.
- [16] A. Cwudziński, J. Jowśa, *SCANMET 2012, Proceedings of 4<sup>th</sup> International Conference on Process Development in Iron and Steelmaking*, June 10-13, Lulea, Sweden, 417-426 (2012).
- [17] A. Cwudziński, J. Jowśa, *ICS 2012, Proceedings of 5<sup>th</sup> International Congress on the Science and Technology of Steelmaking*, October 1-3, Dresden, Germany, 1-6 (2012).

- [18] A. Cwudziński, CSSCR 2013, Proceedings of 3<sup>rd</sup> International Symposium on Cutting Edge of Computer Simulation of Solidification, Casting and Refining, May 20-23, Helsinki, Finland and Stockholm, Sweden, 70 (2013).
- [19] J. Falkus, Archiv. of Metall. and Mater. **41**, 441-454 (1996).
- [20] B.G. Thomas, Continuous Casting **10**, 115-127 (2003).
- [21] M.J. Cho, I.C. Kim, ISIJ Int. **46**, 1416-1420 (2006).

*Received: 4 December 2013.*